Mechanics of Composite Materials, Vol. 51, No. 4, September, 2015 (Russian Original Vol. 51, No. 4, July-August, 2015)

THREE-DIMENSIONAL ANALYSIS OF METAL-CERAMIC SHELLS BY THE METHOD OF SAMPLING SURFACES

G. M. Kulikov* and S. V. Plotnikova

Keywords: *metal-ceramic shell, elasticity theory, method of sampling surfaces*

An efficient method for solving three-dimensional elasticity problems for metal-ceramic composite shells is presented. According to this method, in the shell body, N sampling surfaces (SaS) parallel to its midsurface are chosen in order to introduce the displacement vectors of these surfaces as unknown functions. The SaS pass through the nodes of a Chebyshev polynomial, which improves the convergence of the SaS method significantly. As a result, this method can be applied to the derivation of such analytical solutions for metal-ceramic shells that asymptotically approach the exact three-dimensional solutions of elasticity as the number N of SaS tends to infinity.

Introduction

In the literature, several approaches to the determination of exact solutions of elasticity theory for metal-ceramic composite plates and shells are known. The first approach is based on the application of asymptotic methods [1, 2], and the second one is connected with the use of power series in 3D approximations of the functions and elastic constants required [3-5]. The state of the art of the problem is discussed in reviews [6, 7].

An alternative approach is connected with introduction of N sampling surfaces Ω^1, Ω^2, ..., Ω^N into the body of the shell parallel to its midsurface in order to use the displacements vectors $\mathbf{u}^1$, $\mathbf{u}^2$, ..., $\mathbf{u}^N$ of these surfaces as sought-for functions [8, 9]. Such a choice of required functions, with subsequent employment of the $(N-1)$th-order Lagrange polynomials in three-dimensional approximations of the displacements allows one to present the high-order resolving equations of the suggested

Tambov State Technical University, Russia
*Corresponding author; e-mail: gmkulikov@mail.ru

Translated from Mekhanika Kompozitnykh Materialov, Vol. 51, No. 4, pp. 647-660 , July-August, 2015. Original article submitted September 16, 2014.

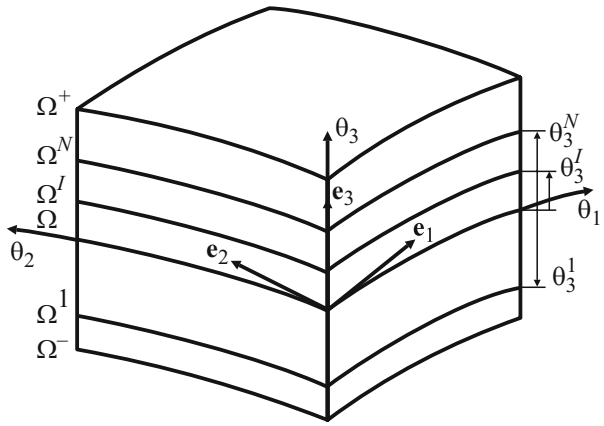

Fig. 1. Arrangement of sampling surfaces in a shell.

theory of shells in a sufficiently compact form and to construct deformation relations exactly representing displacements of the shell as a rigid body in a system of curvilinear surface coordinates [10]. We should note that a second-order theory of shells with three sampling surfaces was constructed in [11].

A high-order theory of shells [8] is based on the use of equidistant sampling surfaces. In this case, faces of a shell are also chosen as sampling ones. This restricts the application of the theory to the calculation of thick shells. The point is that the suggested three-dimensional polynomial interpolation of the displacement vector with the use of Lagrange polynomials of a high degree can lead, owing to the Runge phenomenon, to significant oscillations of polynomial approximations in the zones of edge effect. This phenomenon was discovered by Runge [12] in investigating the error of polynomial interpolation for approximation of some functions on a uniform mesh. With increasing degree of polynomial, the error of interpolation can tend to infinity. In a numerical analysis, to prevent this phenomenon, the roots of a Chebyshev polynomial [13] are usually employed as interpolation nodes, which helps one to significantly improve the behavior of high-degree polynomial approximations, for which the interpolation error uniformly tends to zero at $N \to \infty$. This makes it possible to find solutions to three-dimensional problems of statics for composite shells [14-16] with any preset accuracy, taking into account the fact that the analytical solutions obtained approach the exact solutions of the 3D theory of elasticity asymptotically.

Kinematics of Shell and Deformation Relations

Let us consider a shell of constant thickness h. We relate its midsurface Ω to the curvilinear orthogonal coordinates θ_1 and θ_2 reckoned along the lines of main curvatures and the θ_3 coordinate reckoned in the transverse direction. Let $\mathbf{e}_\alpha$ be the tangential unit vectors of the coordinate lines θ_α, $\mathbf{e}_3$ — the unit vector of the external normal to the midsurface, A_α — coefficients of the first quadratic form, k_α — the principal curvatures, $c_\alpha = 1 + k_\alpha \theta_3$ — components of the geometrical shear tensor, $c_\alpha^I = c_\alpha(\theta_3^I) = 1 + k_\alpha \theta_3^I$ — components of the geometrical shear tensor on the sampling surfaces Ω^I (Fig. 1), and θ_3^I — the transverse coordinates of surfaces Ω^I, which lie in the interval $(-h/2,\ h/2)$, pass through the nodes of an Nth-degree Chebyshev polynomial, and are determined according to the formula [13]

$$\theta_3^I = -\frac{h}{2}\cos\left(\pi \frac{2I-1}{2N}\right). \tag{1}$$

Hereinafter, the indices I, J, and K mark the quantities belonging to the sampling surfaces and taking the values 1, 2, …, N; the Greek subscripts $\alpha, \beta = 1,2$; the Latin subscripts $i, j, k, l = 1,2,3$. Note that, in this study, summation over the repeating Latin indices is assumed.

The components of strain tensor on the sampling surfaces can be written in the vector form [10]

$$2\varepsilon^I_{\alpha\beta} = 2\varepsilon_{\alpha\beta}(\theta^I_3) = \frac{1}{A_\alpha c^I_\alpha}\mathbf{u}^I_{,\alpha}\cdot\mathbf{e}_\beta + \frac{1}{A_\beta c^I_\beta}\mathbf{u}^I_{,\beta}\cdot\mathbf{e}_\alpha,$$

$$2\varepsilon^I_{\alpha 3} = 2\varepsilon_{\alpha 3}(\theta^I_3) = \boldsymbol{\beta}^I\cdot\mathbf{e}_\alpha + \frac{1}{A_\alpha c^I_\alpha}\mathbf{u}^I_{,\alpha}\cdot\mathbf{e}_3, \tag{2}$$

$$\varepsilon^I_{33} = \varepsilon_{33}(\theta^I_3) = \boldsymbol{\beta}^I\cdot\mathbf{e}_3,$$

where $\mathbf{u}^I = \mathbf{u}(\theta^I_3)$ and $\boldsymbol{\beta}^I = \mathbf{u}_{,3}(\theta^I_3)$ are displacement vectors of the sampling surfaces and the derivative of the displacement vector along the θ_3 coordinate on the surfaces Ω^I.

Now, let us present the vectors $\mathbf{u}^I$ and $\boldsymbol{\beta}^I$ in the orthonormalized basis $\mathbf{e}_i$:

$$\mathbf{u}^I = u^I_i\mathbf{e}_i, \tag{3}$$

$$\boldsymbol{\beta}^I = \beta^I_i\mathbf{e}_i. \tag{4}$$

Differentiating Eq. (3) with respect to the transverse coordinate θ_3 and taking into account differentiation formulas for the basis vectors $\mathbf{e}_i$ in curvilinear orthogonal coordinates [10], we obtain

$$\mathbf{u}^I_{,\alpha} = A_\alpha\lambda^I_{i\alpha}\mathbf{e}_i, \tag{5}$$

where

$$\lambda^I_{\alpha\alpha} = \frac{1}{A_\alpha}u^I_{\alpha,\alpha} + B_\alpha u^I_\beta + k_\alpha u^I_3, \quad \lambda^I_{\beta\alpha} = \frac{1}{A_\alpha}u^I_{\beta,\alpha} - B_\alpha u^I_\alpha \quad (\beta\neq\alpha),$$

$$\lambda^I_{3\alpha} = \frac{1}{A_\alpha}u^I_{3,\alpha} - k_\alpha u^I_\alpha, \quad B_\alpha = \frac{1}{A_\alpha A_\beta}A_{\alpha,\beta} \quad (\beta\neq\alpha). \tag{6}$$

Inserting expansions (4) and (5) into Eqs. (2), we come to the scalar form of deformation relations

$$2\varepsilon^I_{\alpha\beta} = \frac{1}{c^I_\beta}\lambda^I_{\alpha\beta} + \frac{1}{c^I_\alpha}\lambda^I_{\beta\alpha}, \quad 2\varepsilon^I_{\alpha 3} = \beta^I_\alpha + \frac{1}{c^I_\alpha}\lambda^I_{3\alpha}, \quad \varepsilon^I_{33} = \beta^I_3. \tag{7}$$

Up to this point, no assumptions about the character of distribution of displacement and strain fields across the shell thickness were made. Now, we assume that the displacements and strains are distributed in the transverse direction according to the following law [8]:

$$u_i = \sum_I L^I u^I_i, \tag{8}$$

$$\varepsilon_{ij} = \sum_I L^I\varepsilon^I_{ij}, \tag{9}$$

where $L^I(\theta_3)$ are the $(N-1)$th-degree Lagrange polynomials, which are defined by the formula

$$L^I = \prod_{J\neq I}\frac{\theta_3-\theta^J_3}{\theta^I_3-\theta^J_3}. \tag{10}$$

From relations (8), we have

$$\beta^I_i = \sum_J M^J(\theta^I_3)u^J_i, \tag{11}$$

where $M^J = L^J_{,3}$ are polynomials of degree $N-2$; their values on the sampling surfaces Ω^I are found from the formulas

$$M^J(\theta^I_3) = \frac{1}{\theta^J_3-\theta^I_3}\prod_{K\neq I,J}\frac{\theta^I_3-\theta^K_3}{\theta^J_3-\theta^K_3} \quad (J\neq I), \tag{12}$$

$$M^I\left(\theta_3^I\right) = -\sum_{J \neq I} M^J\left(\theta_3^I\right). \tag{12}$$

As seen, the determining functions β_i^I of the given high-order theory of shells, according to Eq. (11), are presented as a linear combination of the displacements u_i^J of sampling surfaces.

We should note that deformation relations (6), (7), and (11) exactly represent displacements of the shell as a rigid body in the system of curvilinear surface coordinates. The proof of this fundamental statement is given in [10].

Variational Formulation of the Problem

The principle of minimum potential energy of the shell in the case of conservative loading has the form

$$\delta \Pi = 0, \tag{13}$$

$$\Pi = \frac{1}{2} \iint_{\Omega} \int_{-h/2}^{h/2} \sigma_{ij} \varepsilon_{ij} A_1 A_2 c_1 c_2 d\theta_1 d\theta_2 d\theta_3 - W, \tag{14}$$

$$W = \iint_{\Omega} \left(c_1^+ c_2^+ p_i^+ u_i^+ - c_1^- c_2^- p_i^- u_i^- \right) A_1 A_2 d\theta_1 d\theta_2 + W_{\Sigma}, \tag{15}$$

where Π is the total potential energy of the shell; σ_{ij} are stresses; p_i^- and p_i^+ are the surface loads operating on the faces Ω^- and Ω^+ of the shell; $u_i^- = u_i(-h/2)$ and $u_i^+ = u_i(h/2)$ are the displacements of shell faces; $c_\alpha^- = 1 - k_\alpha h/2$ and $c_\alpha^+ = 1 + k_\alpha h/2$ are the components of shear tensor on these faces; W_Σ is the work of the external loads operating on the lateral surface Σ.

Inserting the distribution of strains in the transverse direction (9) into functional (14) and introducing the resulting stresses

$$H_{ij}^I = \int_{-h/2}^{h/2} \sigma_{ij} L^I c_1 c_2 d\theta_3, \tag{16}$$

we have

$$\Pi = \frac{1}{2} \iint_{\Omega} \sum_I H_{ij}^I \varepsilon_{ij}^I \, A_1 A_2 d\theta_1 d\theta_2 - W. \tag{17}$$

We will restrict ourselves to the consideration of linearly elastic materials, which obey the relations of the generalized Hooke's law,

$$\sigma_{ij} = C_{ijkl} \varepsilon_{kl}, \tag{18}$$

where C_{ijkl} are the elastic moduli of the shell.

The next step consists in the choice of a distribution law for the elastic constants across the thickness of the shell. It is obvious that their distribution in the transverse direction has to agree with the distribution of displacements and strains (8) and (9), i.e., we have

$$C_{ijkl} = \sum_I L^I C_{ijkl}^I, \tag{19}$$

where $C_{ijkl}^I = C_{ijkl}(\theta_3^I)$ are the values of elastic moduli on the sampling surfaces.

Introducing stresses (18) into Eq. (16) and taking into account the distributions of strains (9) and elastic constants (19) across the thickness of shell, we come to the formula for calculating the resulting stresses

$$H_{ij}^I = \sum_{J,K} \Lambda^{IJK} C_{ijkl}^J \varepsilon_{kl}^K, \tag{20}$$

where

$$\Lambda^{IJK} = \int_{-h/2}^{h/2} L^I L^J L^K c_1 c_2 d\theta_3. \tag{21}$$

Elastic Constants of a Metal-Ceramic Composite

Let us consider a composite with a metal matrix and randomly oriented discrete ceramic inclusions serving as reinforcing elements. For the Young's moduli, shear moduli, and Poisson ratios of the metal and ceramics, the standard designations $E_{\mathrm{m}}, G_{\mathrm{m}}, \nu_{\mathrm{m}}$, and $E_{\mathrm{c}}, G_{\mathrm{c}}, \nu_{\mathrm{c}}$ will be used.

We assume that the ceramic inclusions have an ellipsoidal form. Then, the effective elastic moduli of the metal-ceramic composite can be found by using the Mori–Tanaka method [17, 18]:

$$K = K_{\mathrm{m}} + \frac{V_{\mathrm{c}}(K_{\mathrm{c}} - K_{\mathrm{m}})}{1 + V_{\mathrm{m}}(K_{\mathrm{c}} - K_{\mathrm{m}})/(K_{\mathrm{m}} + 4G_{\mathrm{m}}/3)},$$

$$G = G_{\mathrm{m}} + \frac{V_{\mathrm{c}}(G_{\mathrm{c}} - G_{\mathrm{m}})}{1 + V_{\mathrm{m}}(G_{\mathrm{c}} - G_{\mathrm{m}})/(G_{\mathrm{m}} + f_{\mathrm{m}})}, \quad f_{\mathrm{m}} = \frac{G_{\mathrm{m}}(9K_{\mathrm{m}} + 8G_{\mathrm{m}})}{6(K_{\mathrm{m}} + 2G_{\mathrm{m}})}, \tag{22}$$

$$K_{\mathrm{m}} = \frac{E_{\mathrm{m}}}{3(1 - 2\nu_{\mathrm{m}})}, \quad K_{\mathrm{c}} = \frac{E_{\mathrm{c}}}{3(1 - 2\nu_{\mathrm{c}})},$$

where K_{m} and K_{c} are the bulk moduli of elasticity of the metal and ceramics; V_{m} and V_{c} are the volume content of metal and ceramics varying across shell thickness according to the following law [3]:

$$V_{\mathrm{m}} = 1 - V_{\mathrm{c}}, \quad V_{\mathrm{c}} = V_{\mathrm{c}}^{-} + (V_{\mathrm{c}}^{+} - V_{\mathrm{c}}^{-})(h/2 + \theta_3)^{\gamma}, \tag{23}$$

where V_{c}^{-} and V_{c}^{+} are the values of volume content of ceramics on the faces of the shell.

Numerical Results and Discussion

1. As a first example, we will consider a hinged rectangular metal-ceramic plate subjected to a load sinusoidally distributed on its upper surface,

$$p_3^{+} = p_0 \sin\frac{\pi\theta_1}{a} \sin\frac{\pi\theta_2}{b}, \quad p_3^{-} = 0, \tag{24}$$

where $p_0 = 1$ Pa.

The boundary conditions for the rectangular plate with hinged edges are

$$\sigma_{11} = u_2 = u_3 = 0 \text{ at } \theta_1 = 0, \ \theta_1 = a, \tag{25}$$

$$\sigma_{22} = u_1 = u_3 = 0 \text{ at } \theta_2 = 0, \quad \theta_2 = b.$$

To satisfy boundary conditions (25), the solution to the problem will be sought in the form

$$u_1^I = u_{10}^I \cos\frac{\pi\theta_1}{a} \sin\frac{\pi\theta_2}{b}, \quad u_2^I = u_{20}^I \sin\frac{\pi\theta_1}{a} \cos\frac{\pi\theta_2}{b},$$

$$u_3^I = u_{30}^I \sin\frac{\pi\theta_1}{a} \sin\frac{\pi\theta_2}{b}. \tag{26}$$

Inserting load (24) and displacements (26) into the formula for the total potential energy (15) and (17) and taking into account relations (6), (7), (11), and (20), we have

$$\Pi = \Pi(u_{i0}^I). \tag{27}$$

Employing the principle of minimum potential energy (13), (27), we come to the system of linear algebraic equations of order $3N$

$$\frac{\partial \Pi}{\partial u_{i0}^I} = 0, \tag{28}$$

which is solved by the Gauss method.

The algorithm described was realized in the MATLAB programming environment with the use of the ToolBox Symbolic Math package, which allows one to carry out symbolic calculations. As a result, an analytical solution to the problem of bending of a rectangular metal-ceramic plate was obtained on the basis of this high-order theory of shells.

To compare the results obtained with the analytical solution of the three-dimensional problem of elasticity theory [3], we assume that $a = b = 1$ m, $E_{\mathrm{m}} = 7 \cdot 10^{10}$ Pa, $\nu_{\mathrm{m}} = 0.3$, $E_{\mathrm{c}} = 4.27 \cdot 10^{11}$ Pa, $\nu_{\mathrm{c}} = 0.17$, $V_{\mathrm{c}}^- = 0$, $V_{\mathrm{c}}^+ = 0.5$, and $\gamma = 2$ and introduce the dimensionless quantities

$$U_1 = 100h^2 E_{\mathrm{m}} u_1(0, a/2, z)/a^3 p_0, \quad U_3 = 100h^3 E_{\mathrm{m}} u_3(a/2, a/2, z)/a^4 p_0,$$

$$S_{11} = 10h^2 \sigma_{11}(a/2, a/2, z)/a^2 p_0, \quad S_{12} = 10h^2 \sigma_{12}(0, 0, z)/a^2 p_0,$$

$$S_{13} = 10h\sigma_{13}(0, a/2, z)/ap_0, \quad S_{33} = \sigma_{33}(a/2, a/2, z)/p_0, \quad z = \theta_3/h.$$

As seen from the data of Tables 1 and 2, by a proper choice of sampling surfaces, a good coordination between calculated data and the analytical solution [3] can be achieved even for thick metal-ceramic plates. It turned out that the choice of nine sampling surfaces allowed us to obtain numerical results with coincident all five significant digits for the displacements and stresses found in [3]. We should also note that a further increase in the number of sampling surfaces to 19 increased the number of correct significant digits to 11 for the normal stresses and to 15 for the transverse tangential stresses in the case with $a/h = 5$.

2. In a second example, we will consider bending of a hinge-supported cylindrical metal-ceramic shell of radius R and length L. Its midsurface is referred to the curvilinear coordinates θ_1 and θ_2 reckoned in the meridional and circumferential directions. Let the shell be subjected to a load sinusoidally distributed on its external surface,

$$p_3^+ = p_0 \sin\frac{\pi\theta_1}{L}\cos\theta_2, \quad p_3^- = 0, \tag{29}$$

where $p_0 = 1$ Pa.

The boundary conditions for the cylindrical shell with hinged edges are

$$\sigma_{11} = u_2 = u_3 = 0 \text{ at } \theta_1 = 0,\ \theta_1 = L. \tag{30}$$

The solution to the problem satisfying boundary conditions (30) can be sought in the form

$$u_1^I = u_{10}^I \cos\frac{\pi\theta_1}{L}\cos\theta_2, \quad u_2^I = u_{20}^I \sin\frac{\pi\theta_1}{L}\sin\theta_2, \ u_3^I = u_{30}^I \sin\frac{\pi\theta_1}{L}\cos\theta_2. \tag{31}$$

Inserting load (29) and displacements (31) into the formula for total potential energy (15), (17) and employing the principle of minimum potential energy (13), we again arrive at the system of linear algebraic equations (28), which is solved by the Gauss method.

The above-described algorithm was realized in the MATLAB programming environment with the ToolBox Symbolic Math package, which makes it possible to perform symbolic calculations. As a result, an analytical solution of the problem for a metal-ceramic cylindrical shell was derived on the basis of the high-order theory of shells constructed.

TABLE 1. Calculation Results for a Square Metal-Ceramic Plate at $a/h = 5$

N	$U_1(0.5)$	$U_3(0.5)$	$S_{11}(0.5)$	$S_{12}(0.5)$	$S_{13}(0)$	$S_{33}(0.25)$
3	–2.838340262398618	2.491469749603327	2.501382580630834	–1.396928304286311	1.590619403769780	0.7124999023164764
7	–2.912908134299325	2.555878887142974	2.755727774481453	–1.559557127193362	2.310138127165216	0.8099883632143655
11	–2.912918233124032	2.555881463601872	2.756212114487591	–1.559952113334130	2.310019719768843	0.8100152119426805
15	–2.912918241237284	2.555881465062731	2.756213284948613	–1.559953146848270	2.310019478367794	0.8100148488194952
19	–2.912918241248020	2.555881465064410	2.756213287523302	–1.559953149637165	2.310019478154247	0.8100148486775266
23	–2.912918241247832	2.555881465064128	2.756213287528492	–1.559953149644632	2.310019478154246	0.8100148486802695
[3]	–2.9129	2.5559	2.7562	–1.5600	2.3100	0.8100

TABLE 2. Calculation Results for a Square Metal-Ceramic Plate at $a/h = 10$

N	$U_1(0.5)$	$U_3(0.5)$	$S_{11}(0.5)$	$S_{12}(0.5)$	$S_{13}(0)$	$S_{33}(0.25)$
3	–2.875130378136801	2.202396920585996	2.412841121703996	–1.420413278358082	1.601325513211140	0.7367643589818127
7	–2.899724811688270	2.214798606780433	2.641956852342622	–1.552565106480717	2.323954032297057	0.8117297257693006
11	–2.899733978942651	2.214801182167397	2.642395937995539	–1.552891720288181	2.323921893370359	0.8123146819945828
15	–2.899733986752316	2.214801183896660	2.642396888131435	–1.552892592322280	2.323921660091405	0.8123134893082843
19	–2.899733986762826	2.214801183898813	2.642396890147046	–1.552892594687380	2.323921659883698	0.8123134883311503
23	–2.899733986762623	2.214801183898711	2.642396890150937	–1.552892594693696	2.323921659883744	0.8123134883405911
[3]	–2.8997	2.2148	2.6424	–1.5529	2.3239	0.8123

TABLE 3. Calculation Results for a Cylindrical Metal-Ceramic Shell at $R/h = 2$

N	$U_1(0.5)$	$U_2(0.5)$	$U_3(0.5)$	$S_{11}(0.5)$	$S_{22}(0.5)$	$S_{12}(0.5)$	$S_{13}(0)$	$S_{23}(0)$	$S_{33}(0)$
3	–2.142	–4.965	5.418	4.055	1.933	–1.833	5.322	–3.128	0.4697
7	–2.152	–4.985	5.437	4.239	1.973	–1.870	7.795	–4.259	0.4719
11	–2.152	–4.985	5.437	4.239	1.973	–1.870	7.795	–4.254	0.4719
15	–2.152	–4.985	5.437	4.239	1.973	–1.870	7.795	–4.253	0.4719
19	–2.152	–4.985	5.437	4.239	1.973	–1.870	7.795	–4.252	0.4719
23	–2.152	–4.985	5.437	4.239	1.973	–1.870	7.795	–4.252	0.4719

TABLE 4. Calculation Results for a Cylindrical Metal-Ceramic Shell at $R/h = 10$

N	$U_1(0.5)$	$U_2(0.5)$	$U_3(0.5)$	$S_{11}(0.5)$	$S_{22}(0.5)$	$S_{12}(0.5)$	$S_{13}(0)$	$S_{23}(0)$	$S_{33}(0)$
3	–1.505	–4.925	5.352	2.868	1.602	–2.027	4.342	0.5370	0.5771
7	–1.505	–4.938	5.365	2.969	1.647	–2.084	6.965	0.4308	0.4284
11	–1.505	–4.938	5.365	2.969	1.647	–2.084	6.965	0.4313	0.4282
15	–1.505	–4.938	5.365	2.969	1.647	–2.084	6.965	0.4314	0.4282
19	–1.505	–4.938	5.365	2.969	1.647	–2.084	6.965	0.4314	0.4282

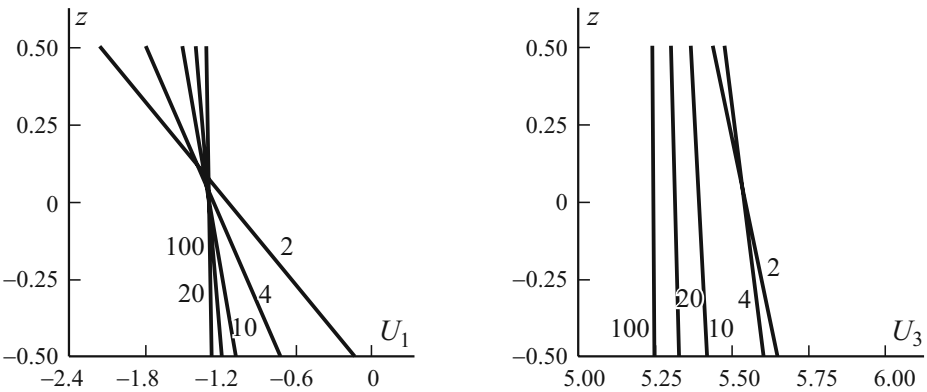

Fig. 2. Distribution of displacements U_1 and U_3 across the thickness of a cylindrical metal-ceramic shell at different values of R/h (numbers at the curves).

It is assumed that the shell is made of a metal-ceramic composite whose mechanical characteristics are given in the previous example. Further, we take that $R = 1$ m, $L = 4$ m, $V_c^- = 0$, $V_c^+ = 0.5$, and $\gamma = 2$ and introduce the following dimensionless quantities:

$$U_1 = hE_m u_1(0,0,z)/R^2 p_0, \quad U_2 = hE_m u_2(L/2,\pi/2,z)/R^2 p_0,$$

$$U_3 = hE_m u_3(L/2,0,z)/R^2 p_0,$$

$$S_{11} = h\sigma_{11}(L/2,\ 0,\ z)/Rp_0, \quad S_{22} = h\sigma_{22}(L/2,\ 0,\ z)/Rp_0,$$

$$S_{12} = h\sigma_{12}(0,\ \pi/2,\ z)/Rp_0, \quad S_{13} = 10R\sigma_{13}(0,\ 0,\ z)/hp_0,$$

$$S_{23} = 100\sigma_{23}(L/2,\ \pi/2,\ z)/p_0, \quad S_{33} = \sigma_{33}(L/2,\ 0,\ z)/p_0, \quad z = \theta_3/h.$$

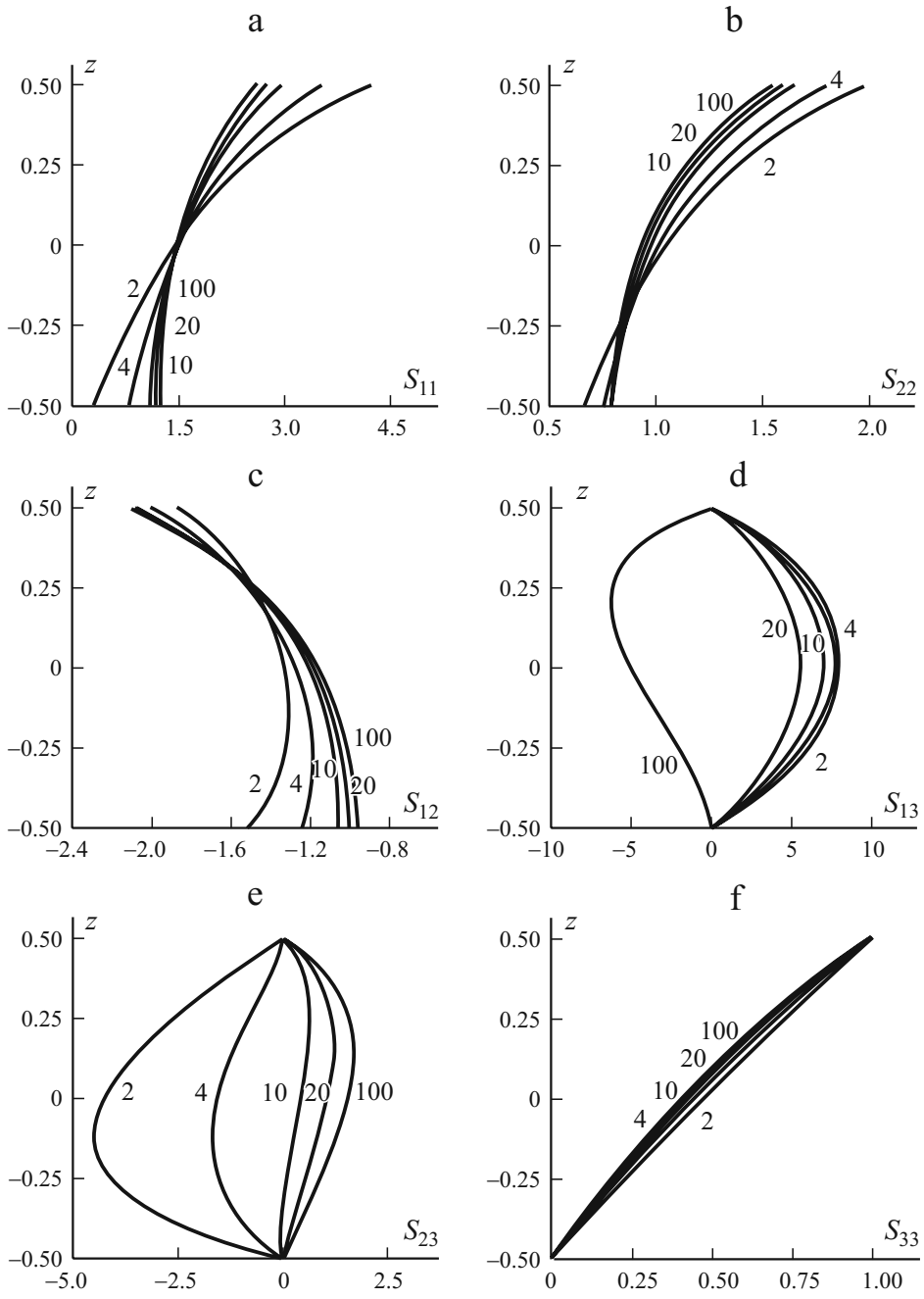

Fig. 3. Distribution of the stresses S_{11}, S_{22}, S_{12}, S_{13}, S_{23}, and S_{33} across the thickness of a cylindrical metal-ceramic shell at different values of R/h (numbers at the curves).

As seen from Tables 3 and 4, the choice of seven sampling surfaces (five will suffice in some cases) yields four correct significant figures almost for all functions, except for the transverse tangential stresses S_{23}, which require a greater number of sampling surfaces. The distribution of displacements and stresses across the thickness of the shell, shown in Figs. 2 and 3 in the case of 11 sampling surfaces chosen for shells with different values of the parameter R/h, also points to the high potential of the theory suggested for calculating metal-ceramic shells in a three-dimensional statement. As seen, the boundary conditions on shell faces for the transverse components of stress tensor are satisfied with a sufficiently high accuracy.

Conclusions

A new method for solving three-dimensional problems of elasticity theory for thick and thin shells made from functional materials is suggested. According to this method, in the shell body, sampling surfaces passing through the nodes of a Chebyshev polynomial are chosen in order to introduce displacement vectors of these surfaces as sought-for functions. This enabled us to find solutions to the three-dimensional problems of statics for metal-ceramic composite shells with any preset accuracy, because the resulting analytical solutions asymptotically approached the exact solutions of the 3D theory of elasticity.

Acknowledgments. This study was financially supported by the Ministry of Education and Science of the Russian Federation (Projects No. 9.137.2014K and No. 339.2014) and the Russian Science Foundation (Project No. 15-19-30002).

REFERENCES

1. Z. Q. Cheng and R. C. Batra, "Three-dimensional thermoelastic deformations of a functionally graded elliptic plate," Composites: Part B, **31**, 97-106 (2000).
2. J. N. Reddy and Z. Q. Cheng, "Three-dimensional thermomechanical deformations of functionally graded rectangular plates," Europ. J. Mech. A/Solids, **20**, 841-855 (2001).
3. S. S. Vel and R. C. Batra, "Exact solution for thermoelastic deformations of functionally graded thick rectangular plates," AIAA J., **40**, 1421-1433 (2002).
4. J. L. Pelletier and S. S. Vel, "An exact solution for the steady-state thermoelastic response of functionally graded orthotropic cylindrical shells," Int. J. Solids Struct., **43**, 1131-1158 (2006).
5. S. S. Vel, "Exact thermoelastic analysis of functionally graded anisotropic hollow cylinders with arbitrary material gradation," Mech. Adv. Mater. Struct., **18**, 14-31 (2011).
6. V. Birman and L. W. Byrd, "Modeling and analysis of functionally graded materials and structures," Appl. Mech. Rev., **60**, 195-216 (2007).
7. D. K. Jha, T. Kant, and R. K. Singh, "A critical review of recent research on functionally graded plates," Compos. Struct., **96**, 833-849 (2013).
8. G. M. Kulikov and S. V. Plotnikova, "Solution of a static problem for an elastic shell in a 3D statement," Dokl. Ross. Akad. Nauk, **439**, No. 5, 613-616 (2011).
9. G. M. Kulikov and S. V. Plotnikova, "A method of solving three-dimensional problems of elasticity theory for laminated composite plates," Mech. Compos. Mater., **48**, No. 1, 15-26 (2012).
10. G. M. Kulikov and S. V. Plotnikova, "Solution of three-dimensional problems for thick elastic shells by using the method of sampling surfaces," Mekh. Tverd. Tela, No. 4, 54-64 (2014).
11. G. M. Kulikov, "Refined global approximation theory of multilayered plates and shells," J. Eng. Mech., **127**, 119-125 (2001).
12. C. Runge, "Über empirische Funktionen und die Interpolation zwischen äquidistanten Ordinaten," Z. Math. Physik, **46**, 224-243 (1901).
13. N. S. Bakhvalov, Numerical Methods. Vol.1 [in Russian], Nauka, Moscow (1973).
14. G. M. Kulikov and S. V. Plotnikova, "On the use of sampling surfaces method for solution of 3D elasticity problems for thick shells," ZAMM — J. Appl. Math. Mech., **92**, 910-920 (2012).
15. G. M. Kulikov and S. V. Plotnikova, "Advanced formulation for laminated composite shells: 3D stress analysis and rigid-body motions," Compos. Struct., **95**, 236-246 (2013).
16. G. M. Kulikov and S. V. Plotnikova, "3D exact thermoelastic analysis of laminated composite shells via sampling surfaces method," Compos. Struct., **115**, 120-130 (2014).
17. T. Mori and K. Tanaka, "Average stress in matrix and average elastic energy of materials with misfitting inclusions," Acta Metallurgica, **21**, 571-574 (1973).
18. Y. Benveniste, "A new approach to the application of Mori–Tanaka's theory in composite materials," Mech. Mater., **6**, 147-157 (1987).